

Supplementary Information

Experimental Methods

Materials Synthesis

1,4-phenylene diisocyanide (PDI) was obtained commercially (Aldrich Chemicals, 99% purity). Phenyl isocyanide was prepared from aniline (Aldrich, 99% purity) *via* the Hofmann carbylamine phase-transfer reaction according to a literature procedure.^{1, 2} The isocyanide was purified prior to use by vacuum distillation at 12 Torr and 52-53 °C to yield a viscous, yellow oil.

Gold Film Preparation and Sample Mounting

Gold nanoparticles were prepared by evaporating gold onto a cleaved mica substrate in a vacuum evaporator (Cooke CVE 301) that was pumped by means of a liquid-nitrogen trapped diffusion pump and operated at a base pressure of $\sim 1 \times 10^{-7}$ Torr. Excess gold (Alfa Aesar, 99.95%) was pre-melted onto tungsten filaments in the thermal evaporator and the samples were prepared by masking the central 5 mm portion of a 1cm \times 1cm mica substrate (highest grade, Ted Pella) with a stainless steel foil, and depositing gold electrode pads ~ 200 nm thick. The mask was removed and the substrates were clamped to a microscope slide using smooth micro-alligator clips which were also connected to vacuum-compatible electrical feedthroughs. Granular thin films were prepared by slowly increasing the evaporator filament voltage to 36 V at a rate that held the filament current to ~ 20 A, at which time the sample conductivity, measured by a Fluke, handheld multimeter, began to increase. Samples were then allowed to age for 12 to 18 hours until the sheet resistance increased to a constant value by 10 to 15 times their original, as-deposited values.

The gold-covered sample was attached to a metal plate affixed to a vacuum-compatible sample manipulator and was in thermal contact with a liquid-nitrogen filled reservoir. After the sample was briefly rinsed with anhydrous benzene (99.8%, Aldrich), the manipulator was inserted into a stainless-steel vacuum chamber that was pumped by means of an ion pump to a base pressure of $\sim 2 \times 10^{-8}$ Torr. The chamber was not baked to avoid altering the sample during bakeout. The temperature was measured by means of a chromel-alumel thermocouple attached to the sample, which reached a base temperature of ~ 90 K with the reservoir filled with liquid nitrogen. The electrical leads to the sample and thermocouple were attached to a vacuum-compatible electrical feedthrough and the I/V characteristics were measured by applying a voltage via a D/A converter and the resulting current measured by means of a Keithly picoammeter that was monitored by an a/d converter to yield I/V curves directly. A diagram of the sample and experimental apparatus is shown in Figure S1

PDI and Phenyl Isocyanide Dosing

1,4-PDI was degassed at room temperature for 1 hour prior to each experiment. Phenyl isocyanide was freeze-pump-thaw degassed for 4 cycles. Both compounds were dosed from a home-built Knudsen source with the sample held at 0 °C and the substrate at room temperature. The gold-covered mica samples were exposed to either PDI or phenyl isocyanide from a directional dosing tube that was incident on the sample which was held at 290 K. This resulted in a local pressure at the sample that was much higher than the background pressure increase.

However, the increase in background pressure while dosing phenyl isocyanide ($\sim 6 \times 10^{-6}$ Torr) was much larger than with PDI ($\sim 1 \times 10^{-9}$ Torr) so that the local pressure at the sample was ~ 6000 times higher for phenyl isocyanide than PDI. It was thus not possible to establish the true exposure (in Langmuirs = 1×10^{-6} Torr s) and exposures are thus quoted as dosing times in Figs. 3 and S3.

Measurement of Temperature-Dependent I/V Curves

I/V curves were measured following each reactant exposure. Temperature-dependent I/V curves were measured as described above by initially cooling the sample to 90 K and then by allowing the liquid nitrogen in the trap to boil away leading to a slow increase in temperature.

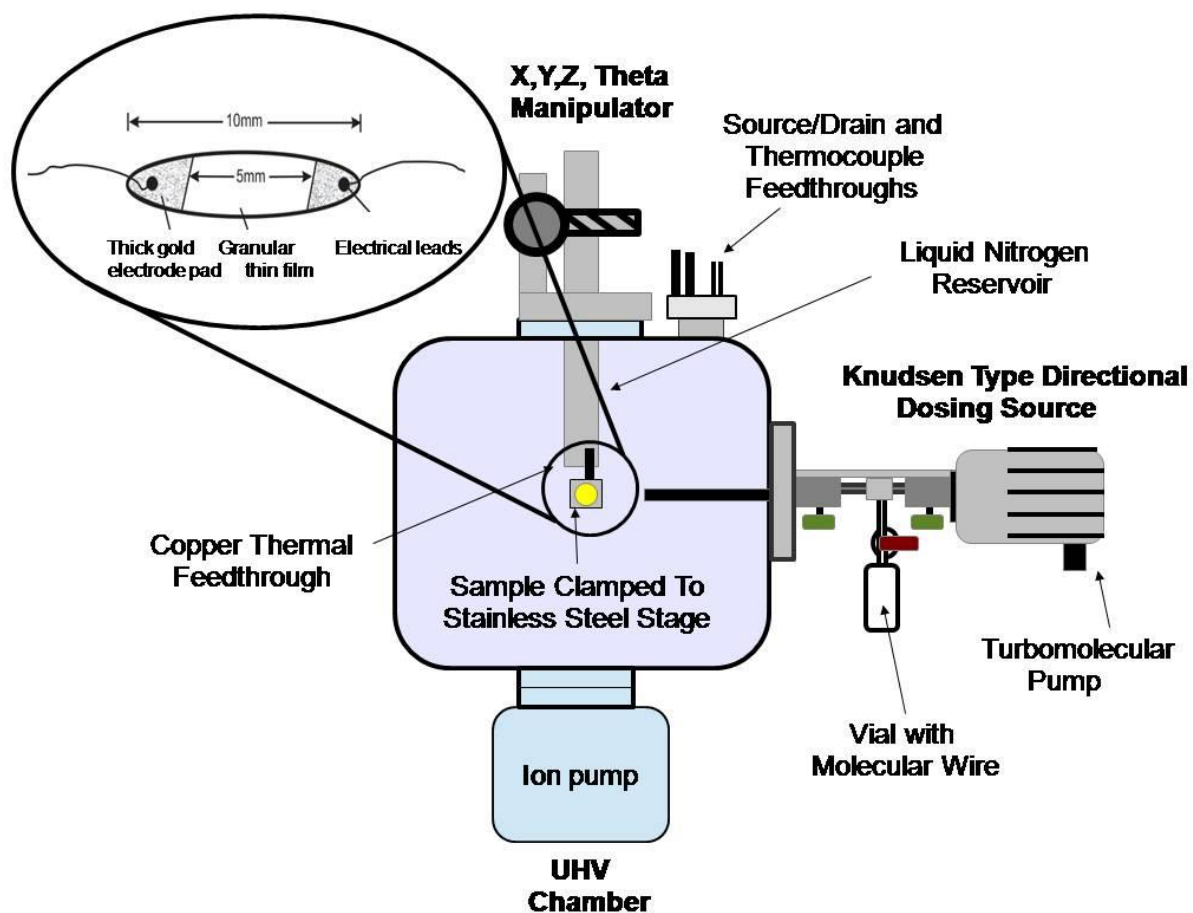
Atomic Force Microscopy and Scanning Tunneling Microscopy

Atomic force microscopy (AFM) images of gold-nanoparticle covered mica surfaces were collected in air using a Pacific Nanotechnology instrument in tapping mode. Pacific Nanotechnology, close-contact, mounted cantilever probes were used and they were tuned between experiments and the cantilever drive amplitude set for soft contact. The mica substrates were anchored to glass microscope slides using double-sided tape.

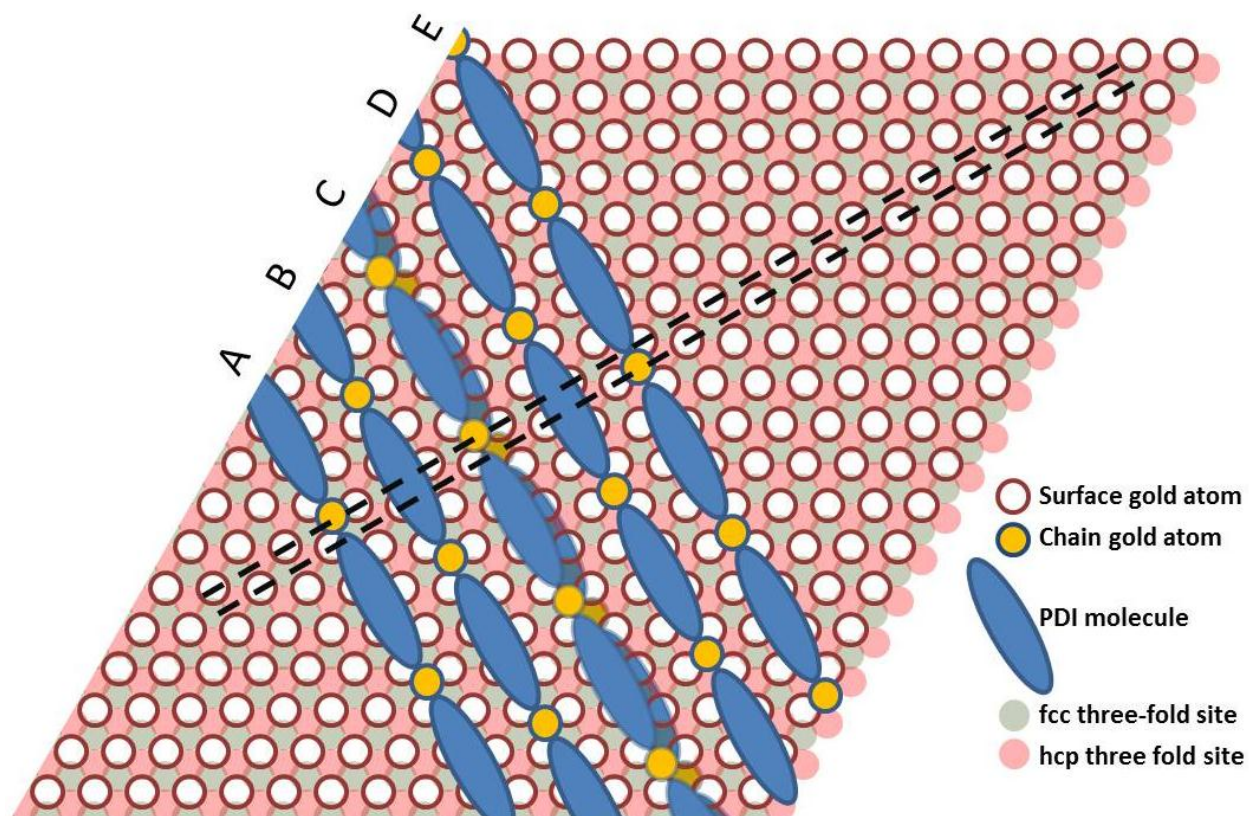
Scanning tunneling microscopy (STM) images of PDI on a Au(111) single crystal surface were collected in an ultrahigh-vacuum (UHV) chamber operating at a base pressure of 2×10^{-10} Torr following bakeout.³ The Au(111) single crystal (Princeton Scientific) was cleaned by using cycles of ion bombardment with 1 keV argon ions for 30 minutes ($1 \mu\text{A}/\text{cm}^2$), annealing to 900 K for 5 minutes and then to 600 K for 30 minutes until cleanliness was verified by obtaining a perfectly defined herringbone reconstruction by STM.^{4,5} The gold surface was exposed to PDI from a directional doser pointed towards the sample held at 300 K and the STM images were acquired at the same temperature. Experiments were performed using a scanning tunneling microscope (RHK UHV 350 dual AFM/STM) as described elsewhere,³ along with the methods used to prepare the tungsten tip.

The STM images of the gold-nanoparticle-covered samples were obtained in air using a RHK UHV 350 dual AFM/STM, in air.

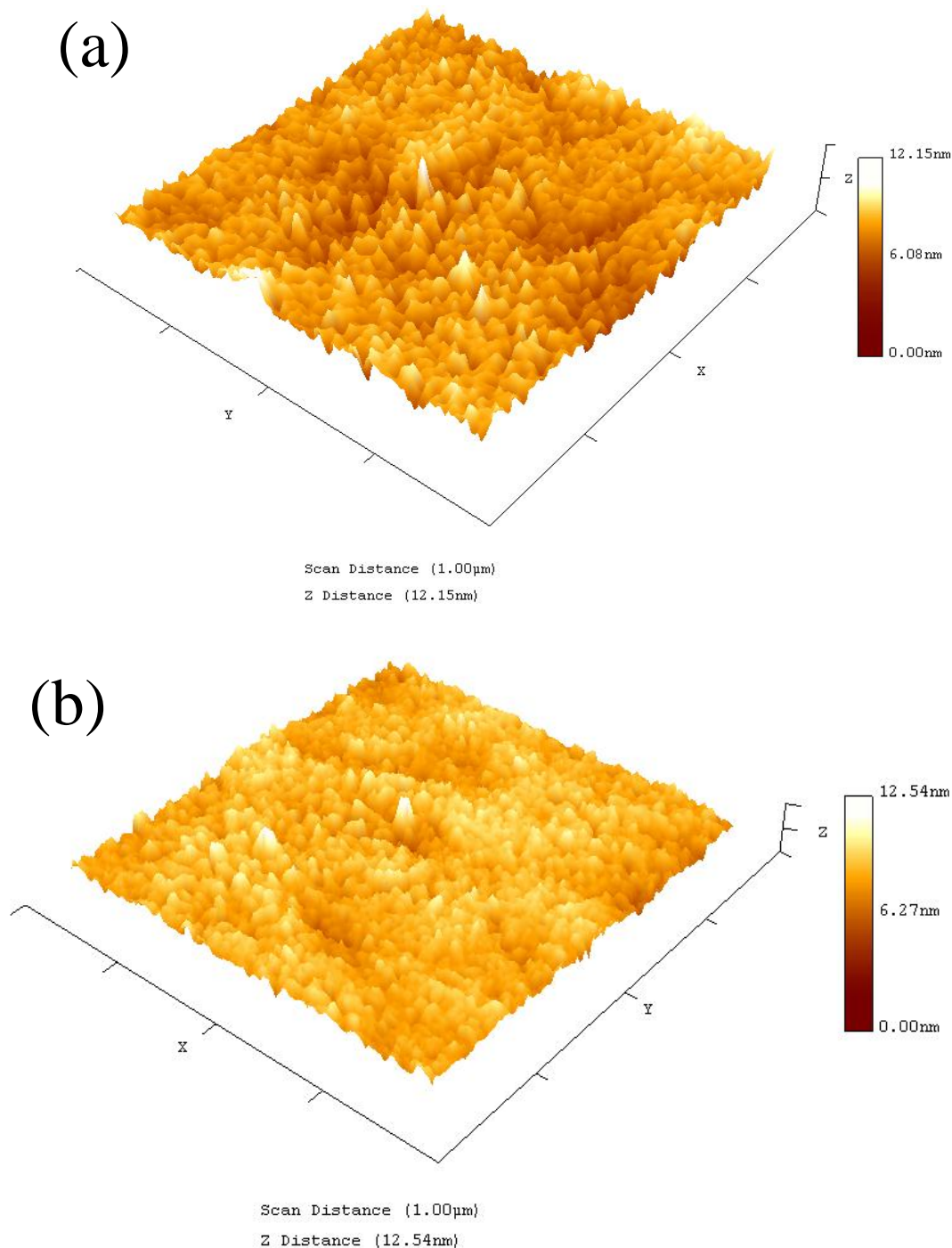
Supplementary Figures



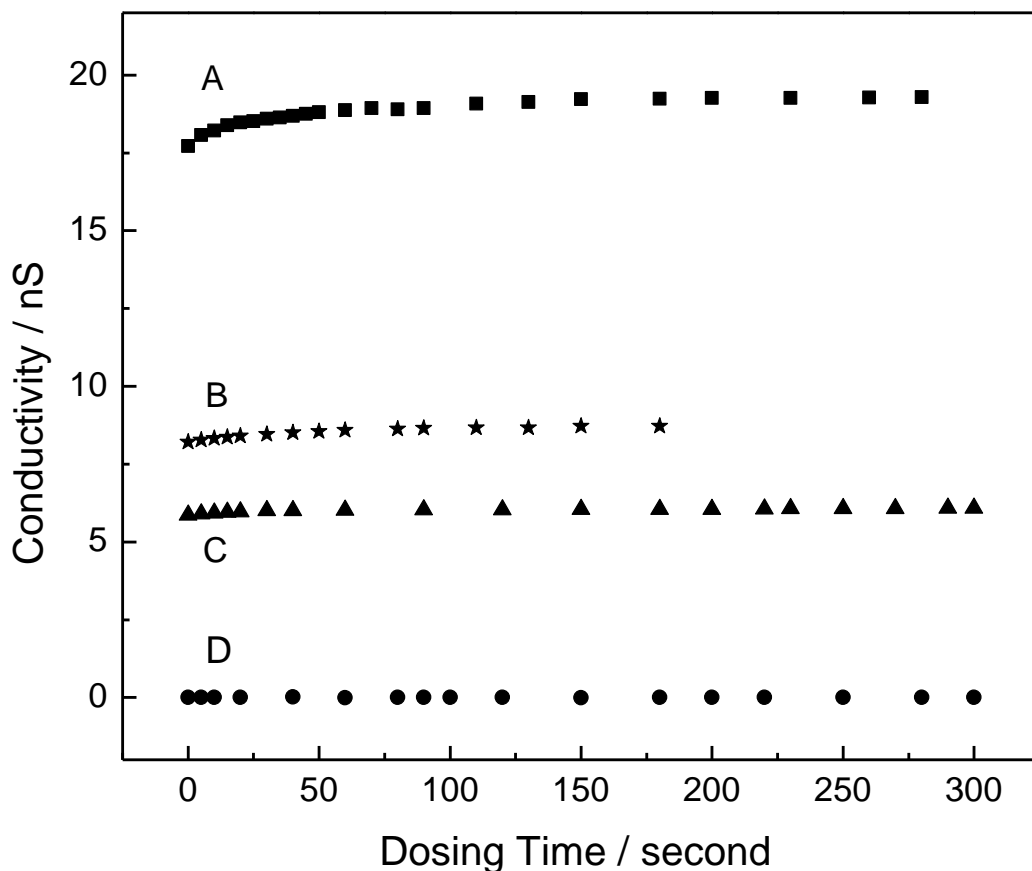
Supplementary Figure 1. Diagram showing the experimental vacuum chamber and the sample used for making the electrical measurements.



Supplementary Figure 2. Depiction of the proposed surface structures of Au-PDI oligomers on a Au(111) substrate. Chains A and B run along hexagonal close packed (hcp)-sites, while chains D and E are located on face-centered cubic (fcc)-sites. Considering that chains with gold atoms located at both kinds of sites have almost identical energies, chain C can be located in two equivalent configurations and it is possible that it can also hop between these two states.

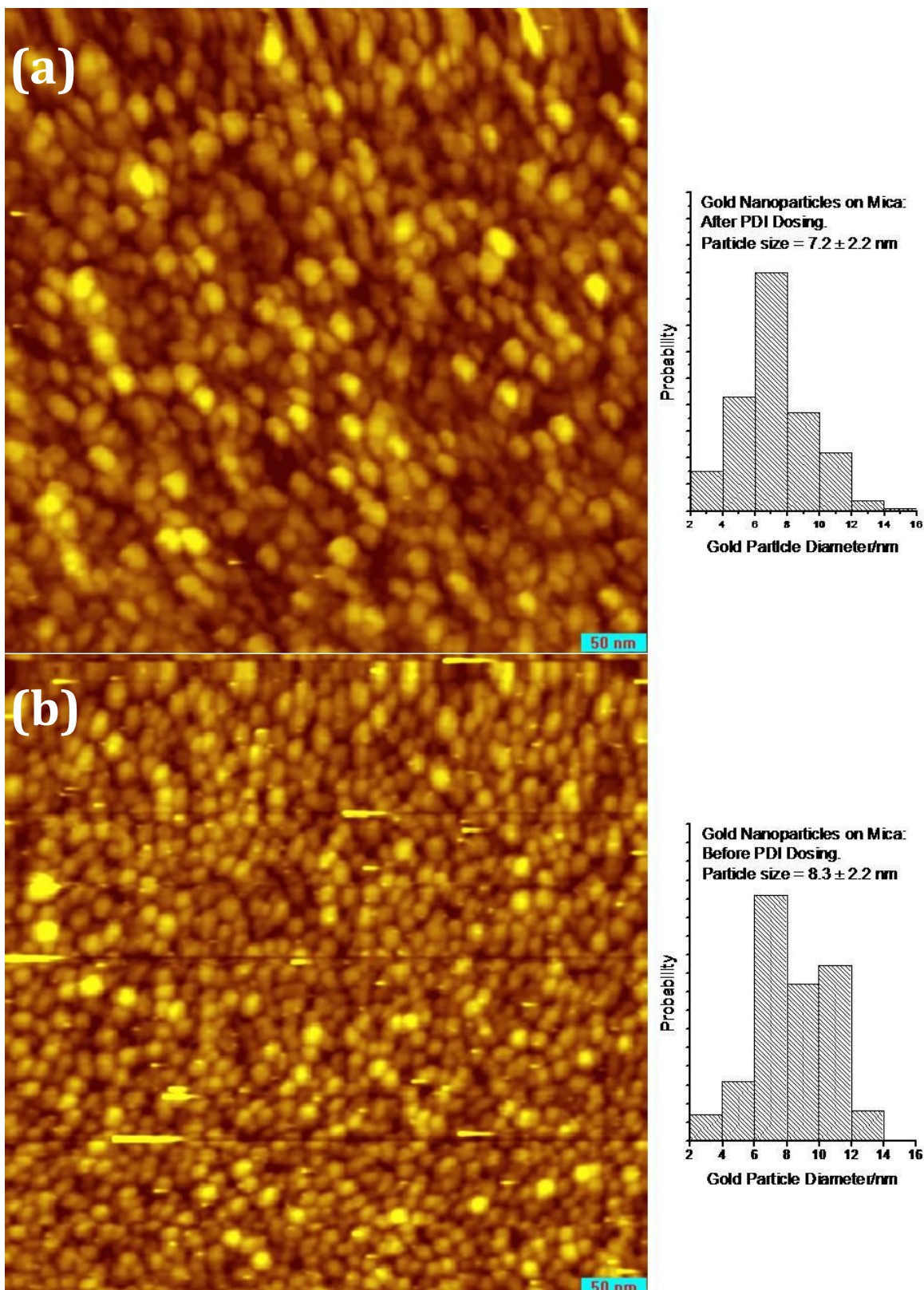


Supplementary Figure 3. Tapping-mode AFM images of gold nanoparticle films formed by evaporating gold onto a mica substrate, (a) with a high initial resistance of 312 M Ω and (b) with a low initial resistance of 48 M Ω . Similar images are obtained for all films (data not shown). In the case of the film with the highest resistance (Fig. S3(a)), the number of particles is $3.3 \pm 0.1 \times 10^{15} / \text{m}^2$, while for the lowest-resistance film (Fig. S3(b)), it is $3.2 \pm 0.1 \times 10^{15} / \text{m}^2$, indicating that the gold nanoparticle density remains constant and the particles increase in size as more gold is added.

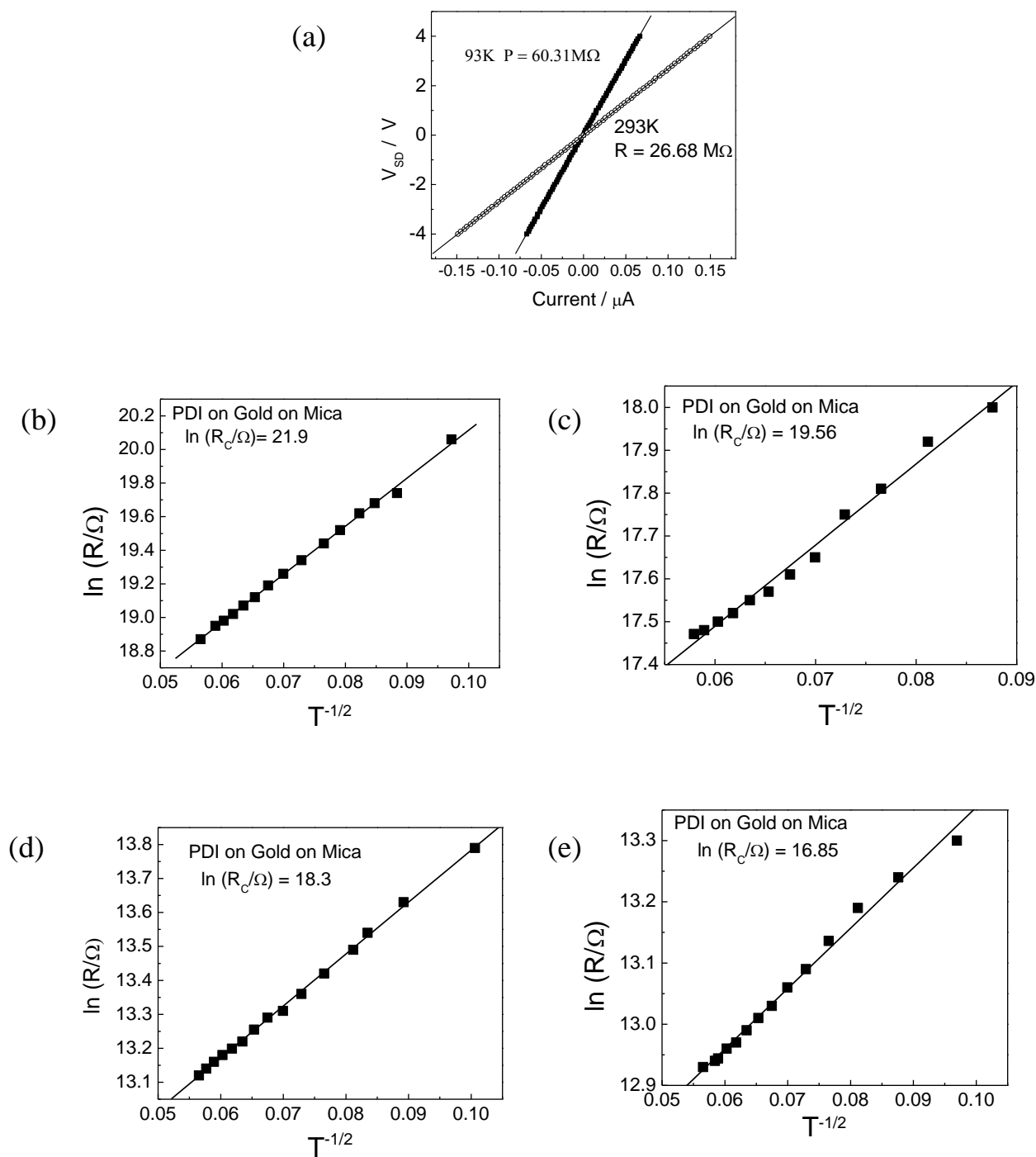


Supplementary Figure 4. Plot of the change in conductivity of a gold film deposited onto mica exposed to phenyl isocyanide from a collimated source as a function of dosing time, where the initial conductivity of the metal films is A, 17.72nS; B, 8.20nS and C, 5.86nS. As indicated above, the dosing pressures for phenyl isocyanide are estimated to be ~600 times larger than for PDI. Note that no significant change in conductivity is found for dosing times for which the PDI causes more than an order of magnitude change in conductivity (Fig. 3)

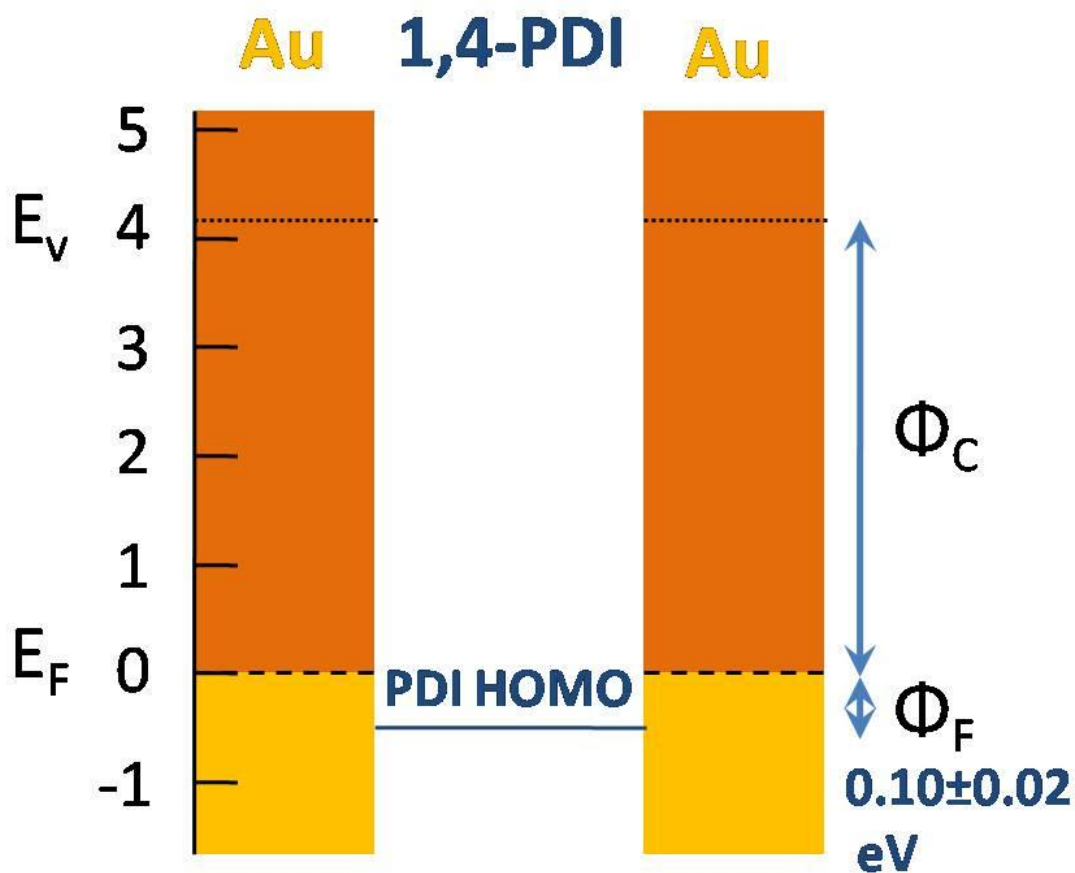
Plot D shows the change in conductivity for a mica film without gold exposed to 1,4-PDI as a function of dosing time, where no detectable change in conductivity is found, while a significant change is found when the gold-covered surface is dosed with PDI. Both gold and diisocyanides are needed to obtain the conductivity change shown in Fig. 3.



Supplementary Figure 5: STM images of gold nanoparticles on mica (a) before PDI (particle density = $3.4 \pm 0.2 \times 10^{15} \text{ m}^{-2}$) and (b) after exposure to PDI (particles density = $3.8 \pm 0.2 \times 10^{15} \text{ m}^{-2}$). $V_t = -1.00 \text{ V}$, $I_t = 8.85 \text{ pA}$. The insets show the size distributions of the gold nanoparticles.



Supplementary Figure 6. (a) Typical I/V curves collected at 93 and 293 K, showing the Ohmic behavior and typical plots of $\ln(R/\Omega)$ versus $1/\sqrt{T}$, where the temperature is measured in degrees Kelvin, for various films with a range of initial films resistances. The values of $\ln(R_C/\Omega)$ are (b) 21.9, (c) 19.56, (d) 18.3 and (e) 16.85.



Supplementary Figure 7. Energy level diagram for gold nanoparticles linked by 1,4-PDI oligomers, where ϕ_C corresponds to the work function of the 1,4-PDI-covered gold nanoparticles (4.08 eV)⁶ and ϕ_F is the tunneling barrier through the linker, measured to be $0.10 \pm 0.02 \text{ eV}$.

Abeles Model for the Relationship between α and $\ln(R_C)$

The Abeles model for thermally assisted tunneling through an array of nanoparticles predicts that the sheet resistance R is given by: $R = R_0 \exp(+2\sqrt{C/kT})$ where $C = \chi s E_c^0$, s is the average spacing between particles, $\chi = \sqrt{2m\phi/\hbar^2}$, ϕ is the height of the tunneling barrier, m is the electron mass, E_c^0 is the Coulomb charging energy, and R_0 a constant.⁷

The variable C can be written as $C = \frac{4\chi e^2}{\epsilon} f(s, d)$, where s is the distance between particles of diameter d , and $f(s, d) = \frac{(s/d)^2}{(\frac{1}{2} + (s/d))}$.^{7, 8} The geometry of the gold nanoparticles is unaffected by PDI dosing (Fig. S4) but does vary with initial gold thickness, producing different initial resistances for each film. Thus, the resistance, R_C , of the clean gold film (prior to dosing with PDI) provides a convenient parameter for describing its properties and is:

$$\ln R_C = \ln R_C^0 + 2\sqrt{\frac{C_C}{300k}} \quad (1)$$

where $T = 300$ K, the temperature at which the resistance was measured.^{7, 8} Taking $\epsilon = 1$ for a vacuum and substituting for C yields:

$$\ln R_C = \ln R_C^0 + \sqrt{\frac{e^2 f(s, d)}{k}} \times \sqrt{\frac{4}{75}} \times \sqrt{\chi_C} \quad (2)$$

In the case of a PDI-covered film, the slopes of plots of $\ln(R)$ versus $1/\sqrt{T}$ (α , Fig. S6) are found to vary linearly with $\ln(R_C)$ (Fig. 4). Since $\alpha = 2\sqrt{\frac{C_F}{k}}$,^{7, 8} where $C_F = \frac{4\chi_F e^2 f(s, d)}{\epsilon_F}$, α is given by:

$$\alpha = \sqrt{\frac{16\chi_F e^2 f(s, d)}{\epsilon_F}} \quad (3).$$

Since $f(s, d)$ is identical for clean and PDI-covered films (Fig. S5), rearranging equation (3) and substituting into equation (2) gives a relationship between α (the slope of plots of $\ln(R)$ versus $1/\sqrt{T}$, Fig. S6) and the initial resistance of the clean film (R_C) (Fig. 4) as:

$$\alpha = 17.32 \sqrt{\frac{\chi_F}{\epsilon_F \chi_C}} \times \ln R_C - 17.32 \sqrt{\frac{\chi_F}{\epsilon_F \chi_C}} \times \ln R_C^0 \quad (4).$$

1. *Organic Syntheses, Coll.*, 1988, **6**, 2.
2. *Organic Syntheses, Coll.*, 1976, **55**, 2.
3. J. A. Boscoboinik, F. C. Calaza, Z. Habeeb, D. W. Bennett, D. J. Stacchiola, M. A. Purino and W. T. Tysoe, *Physical Chemistry Chemical Physics*, 2010, **12**, 11624-11629.
4. J. V. Barth, H. Brune, G. Ertl and R. J. Behm, *Physical Review B*, 1990, **42**, 9307-9318.
5. C. Woll, S. Chiang, R. J. Wilson and P. H. Lippel, *Physical Review B*, 1989, **39**, 7988-7991.
6. J. Zhou, D. Acharya, N. Camillone, P. Sutter and M. G. White, *The Journal of Physical Chemistry C*, 2011, **115**, 21151-21160.
7. B. Abeles, P. Sheng, M. D. Coutts and Y. Arie, *Advances in Physics*, 1975, **24**, 407-461.
8. P. Sheng, B. Abeles and Y. Arie, *Phys. Rev. Lett.*, 1973, **31**, 44-47.